Improvement of in-vivo en-face OCT retinal images using adaptive optics

D. Merino[a], A. Bradu[b], C. Dainty[a] and A. Podoleanu[b]

[a]National University of Ireland Galway, University Road, Galway, Ireland
[b]University of Kent at Canterbury, Canterbury, CT2 7NH, UK

ABSTRACT

A system that is able to obtain *in-vivo* human retinal images using *en-face* optical coherence tomography is presented. The system also includes an adaptive optics closed-loop system that uses a Shack-Hartmann wavefront sensor and a 37 OKO membrane deformable mirror to correct for ocular aberrations. The system has been used to produce *en-face* images of retinal pigment epithelium and the nerve fiber layer collected from several volunteers.

Keywords: *en-face* optical coherence tomography

1. INTRODUCTION

The human retina is an extremely complex structure that is formed by six different types of neuron cells and ten histological layers found in a depth of a few hundred microns. Imaging the retina is a useful tool in order to detect any disease or defect that may affect its performance. Optical coherence tomography (OCT)[1] is a technique based in low coherence interferometry[2,3] that is able to reconstruct tomographic (sectional) images of the object under study. It is usually implemented as a Michelson interferometer, in which the pattern of interference between the reference and object arm is used to determine the amount of light reflected back from a certain point within the volume of the object under study. A broad band source is used for illumination, thus the two beams will only produce an interference pattern when their optical paths differ by less than the coherence length of the source. Lateral resolution obtained using OCT for *in-vivo* retinal imaging is around 10 μm, and depends on the spot size of the probing beam focused in the patient's retina. Depth resolution only depends on the light source used and it can reach values of just a few microns depending on the light source used.

The performance of this technique is clearly limited by the aberrations of the patient's eye, since the images are obtained through the optics of the eye. These aberrations vary widely between subjects,[4] and they are not constant in time.[5] Adaptive optics (AO) has been demonstrated a suitable method to correct for these aberrations[6] and has been used in combination with OCT to improve its performance.[7,8] An increase in the signal-to-noise ratio (SNR) of about 10 dB has been reported using AO-OCT.

Due to the use of longitudinal scanning to obtain traditional OCT images, these lie on a plane parallel to the optical axis and either the x or y axis (longitudinal images), i.e., they lie in a plane perpendicular to that of the retina. Sometimes this is inconvenient since the images cannot be compared with those obtained using other techniques, such as confocal scanning laser ophthalmoscope (SLO),[9] in which the images from a plane perpendicular to the optical axis of the patient's eye are obtained. In *en-face* OCT two scanning mirrors are used to move the focused probing beam over the surface of the object under study to be imaged. The scanning itself introduces the phase modulation between the reference and probing beams necessary to obtain *en-face* OCT images. The scanning configuration in *en-face* OCT is very similar to that used in SLO and this makes it possible to compare images obtained with both techniques.

In this article a system is presented that is able to obtain *en-face* images from the *in-vivo* human retina using *en-face* OCT technology. The system performance has been enhanced by means of AO technique as described below.

5th International Workshop on Adaptive Optics for Industry and Medicine, edited by Wenhan Jiang,
Proc. of SPIE Vol. 6018, 601802, (2005) · 0277-786X/05/$15 · doi: 10.1117/12.669238

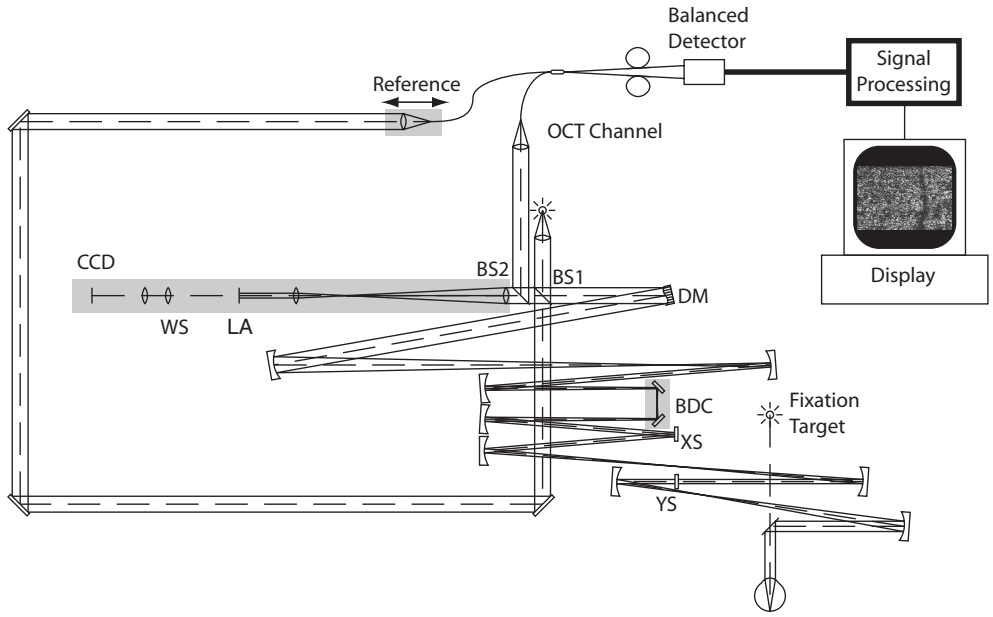

Figure 1. Schematic drawing of the AO-OCT system; BS (beam splitter), DM (deformable mirror), BDC (Badal defocus corrector), XS (X scanner), YS (Y scanner), LA (lenslet array), WS (wavefront sensor)

2. SYSTEM DESCRIPTION

Fig. 1 shows a schematic drawing of the AO-OCT system. The system uses a superluminescent diode (SLD) that has a central wavelength of 830.7 nm, and a bandwidth of 17 nm, which translates into a depth resolution of about 13 μm in the eye. The beam coming from the source is collimated and then split by a beam splitter (90 %T/10 %R, BS1 in the figure) into the reference and probing beams. The probing beam reaches the deformable mirror (DM), a Badal defocus corrector (BDC) and the x or line (XS) and y or frame (YS) scanners before entering the patient's eye. The frequencies at which the scanners work are 2 Hz for the frame scanner and 700 Hz for the line scanner. There are a series of telescopes between these elements formed by pairs of spherical mirrors. Mirrors have been chosen rather than lenses to avoid reflections from their surfaces that may affect the performance of the wavefront sensor (WS). These telescopes change the diameter of the beam in order to fit its size to the dimensions of the elements mentioned above. The diameter of the probing beam is 6mm in the patient's pupil plane. The telescopes also ensure that the patient's pupil plane is conjugate to the XS, YS and DM planes.

The light power reaching the cornea of the patient is 300μW, which is below the threshold dictated in[10] for a non-scanning beam at 830.7 nm. The light scattered back from the patient's retina passes a second time through the object arm, and reaches the second beam splitter (1 %T/99 %R BS2 in Fig.1). Light transmitted through BS2 is collected by the WS. This has been implemented as a Shack-Hartmann wavefront sensor and is described in more detail in the following section of this paper.

The light reflected in BS2 is injected into a single mode fiber optics, that is coupled with the fiber that collects the light from the reference arm and the two beams interfere. The two fibers coming from the coupler are connected to a balanced detector. The signal is then processed for display. The last focusing element and the fiber end in the reference arm are fixed on top of a translation stage, which can be moved 2.5 cm along the optical axis. This introduces the capability of depth scanning in the OCT channel. In this sense, by stopping the frame scanner, and moving the translation stage, images of longitudinal scans of the retina can be obtained, as

Further author information: (Send correspondence to D.M.)
D.M.: E-mail: david.merino@nuigaway.ie
A.B.: E-mail: a.bradu@kent.ac.uk

with traditional OCT systems. In this case, and unlike traditional OCT systems, the fast direction of scanning is perpendicular to the optical axis, while the slow scanning is performed along the optical axis.

3. ADAPTIVE OPTICS SYSTEM DESCRIPTION

The AO system implemented consists of a Shack-Hartmann wavefront sensor (WS) that works in closed-loop together with a deformable mirror from Flexible Optics (OKO Technologies). An array of square lenslets of 200 μm pitch are used in the WS. The lenslets are magnified so their pitch in the patient's pupil is 390 μm on that plane. Thus for a patient's pupil of 6 mm there are around 120 sub-apertures. The system is able to measure and correct the patient's aberrations at a frame rate of 9 fps. This frame rate is limited by the exposure time of the CCD camera used in the WS. Since the images are obtained at a rate of 2 fps (this is the frequency of operation of the frame scanner), the aberration is measured and corrected 4 times for each image obtained. This translates to a bandwidth of 1.3 Hz for the AO system, estimated as suggested in.[11]

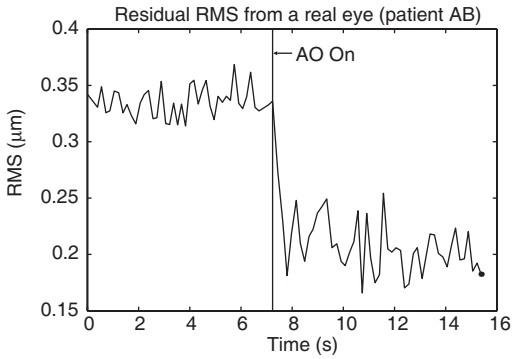

Figure 2. Evolution of the reconstructed RMS when the AO closed-loop system is turned on

Fig. 2 shows the evolution of the reconstructed RMS for a real eye when the AO is turned on. The system is able to reduce the wavefront RMS to a value of around 0.2μm for this particular patient. This value is in good agreement with previous reports using the same deformable mirror.[12]

Fig. 3 shows the measured point spread functions (PSF) before and after correction for an artificial eye. These PSF images have been obtained by blocking the OCT channel using a removable mirror that sends the light to a CCD camera where the beam is focused through a lens and a microscope objective. When no adaptive correction is applied, the RMS of the reconstructed wavefront was 0.15 μm. When adaptive correction was applied the residual RMS was 0.07 μm.

4. RESULTS

The AO-OCT system described above was used to image the retina of several healthy volunteers that did not require previous correction for defocus or astigmatism. The images obtained have different sizes depending on the scanning angle. Also, using the fixation target, different areas of the retina can be imaged.

The effect of AO on the OCT signal has been characterized by using several different parameters. First, an increase on the light intensity injected into the fiber optics is expected, since on the focused beam more energy is concentrated over a smaller area when adaptive correction is applied. An increase of the light intensity has been measured of around 17% when the adaptive correction is applied.

Due to the reduction of the wavefront aberration, an increase in the SNR is expected, as reported in.[7,8] Such behavior has been observed, although it is highly dependent on the subject. The increase on the SNR for the OCT channel is of 4 to 5 dB.

Fig. 4 shows two longitudinal OCT images, to compare the results obtained with and without dynamic correction. The images show how the OCT signal for the retinal pigment epithelium (RPE) and nerve fiber

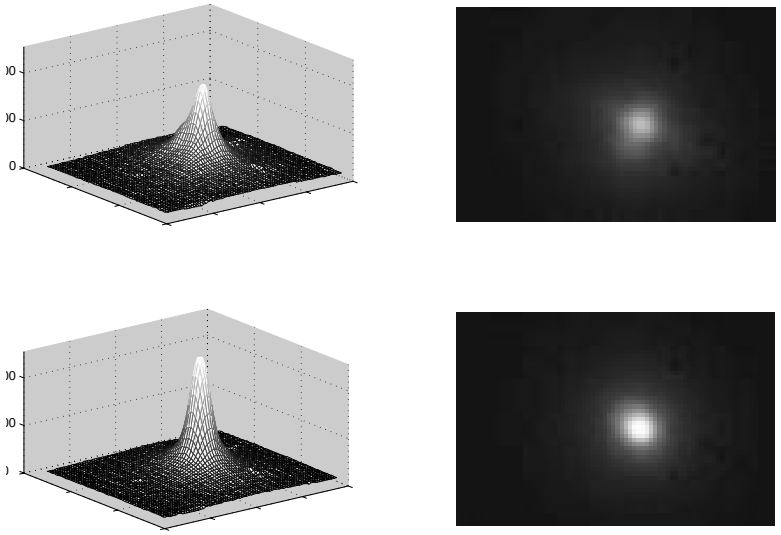

Figure 3. Measured PSF's for an artificial eye without (a) and with (b) adaptive correction

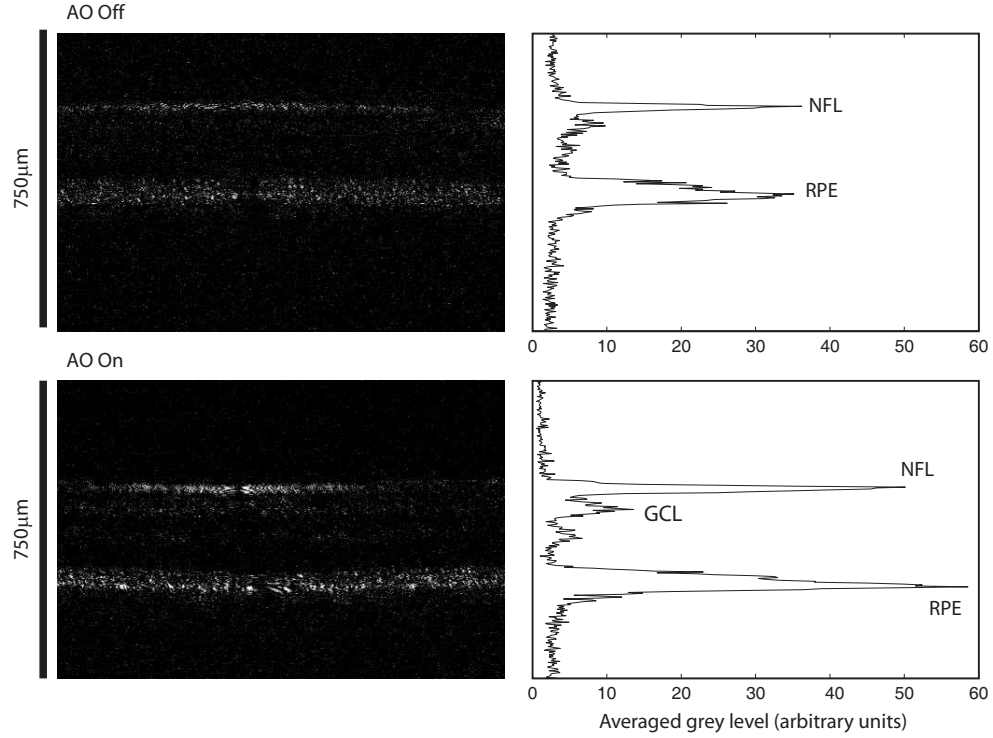

Figure 4. Longitudinal OCT images obtained from patient AB before and after applying adaptive correction. The graphs on the right show the grey level of the image averaged along its x axis. The nerve fiber layer (NFL) and retinal pigment epithelium (RPE) are easily identified in both images, while the ganglion cell layer (GCL) is more easily identifiable with AO.

layer (NFL) is higher when adaptive correction is applied. It also shows how layers that were almost masked by noise become more visible with AO, that is the case of the layer labelled as the ganglion cell layer (GCL). The longitudinal resolution of the images has been measured before and after adaptive correction was applied analyzing the frequency components in the Fourier transform of the image. The longitudinal resolution is 13.6μm without adaptive correction and 13.1μm with it.

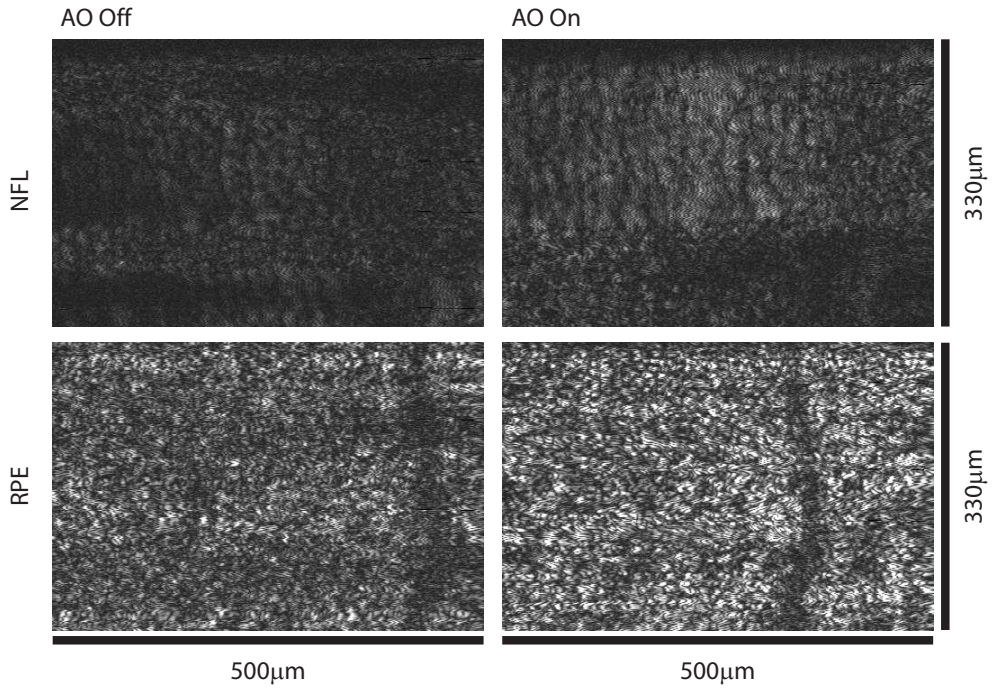

Figure 5. *En-face* OCT images obtained from the same area of patient DM's retina, before and after applying adaptive correction for the RPE and the NFL

Fig. 5 shows two pairs of *en-face* images for two different layers of the volunteer's retina before and after adaptive correction was applied. The top pair of images correspond to the NFL. Due to movements of the patient while the image was acquired the layer is not visible within the whole image. Since the image is taken at 5 deg in the nasal direction, the structure shown oriented in the vertical axis of the image is compatible with the nerve structure expected on that layer. The bottom pair of images show the RPE in the same area of the retina. Since this layer is thicker, the movements of the volunteer are not so obvious here. The structure shown in this case is compatible with the photoreceptor mosaic. An increase in the resolution of the images has been measured when the adaptive correction is applied. To assess this increase we calculated the power spectral density (PSD) of the images obtained. The spatial frequency f for which the volume under the PSD curve within a circle of radius f is 99% of the total volume under the PSD curve was determined. Using this criterion, an increase on the resolution of the images has been detected, showing 6.5 μm before and 5 μm after applying adaptive correction.

5. CONCLUSION

A system has been presented that combines AO and *en-face* OCT, and is able to obtain images from different layers of the *in-vivo* human retina. From a comparative study of commercially available low-cost deformable mirrors,[12] we know that other mirror technologies will yield greatly improved performance of the adaptive optics loop compared to this initial study using the 37 elements OKO MMDM. The images obtained allow the identification of individual cells on the RPE. Other layers have been identified using longitudinal images obtained with the same system. The system represents a step forward towards imaging other kinds of cells in the *in-vivo* human retina, such as ganglion cells.

ACKNOWLEDGMENTS

This research was supported by Science Foundation Ireland under Grant 01/PI.2/B039C.

REFERENCES

1. D. Huang, E. A. Swanson, C. P. Lin, J. S. Schuman, W. G. Stinson, W. Chang, M. R. Hee, T. Flotte, K. Gregory, C. A. Puliafito, and J. G. Fujimoto, "Optical coherence tomography," *Science* **254**, pp. 1178–1181, 1991.
2. S. A. Al-Chalabi, B. Culshaw, and D. E. N. Davies, "Partially coherent sources in interferometric sensors," *First International Conference on Optical Fibre Sensors* , 1983.
3. R. C. Youngquist, S. Carr, and D. E. N. Davies, "Optical coherence-domain reflectometry: A new optical evaluation technique," *Opt. Lett.* , pp. 158–160, 1987.
4. S. Marcos, S. A. Burns, P. M. Prieto, and B. B. R. Navarro, "Investigating sources of variablity of monochromatic and transverse chromatic aberrations across the eye," *Vision Res.* **41**, pp. 3861–3871, 2001.
5. H. Hofer, P. Artal, B. Singer, J. L. Aragón, and D. R. Williams, "Dynamics of the eye's aberration," *J. Opt. Soc. Am. A* **18**, pp. 497–506, 2001.
6. J. Liang, D. R. Williams, and D. T. Miller, "Supernormal vision and high-resolution retinal imaging through adaptive optics," *J. Opt. Soc. Am. A* **14**, pp. 2884–2892, 1997.
7. B. Hermann, E. J.Fernández, A. Unterhuber, H. Sattmann, A. F. Fercher, and W. Drexler, "Adaptive-optics ultrahigh-resolution optical coherence tomography," *Opt. Lett.* **29**, pp. 2142–2144, 2004.
8. Y. Zhang, J. Rha, R. S. Jonnal, and D. T. Miller, "Adaptive optics parallel spectral domain optical coherence tomography for imaging the living retina," *Opt. Express* **13**, pp. 4792–4811, 2005.
9. R. H. Webb, G. W. Hughes, and F. C. Delori, "Confocal scanning laser ophthalmoscope," *Appl. Opt.* **26**, p. 1492, 1987.
10. *Safety of Laser Products*, The European Comitee for Electrotechnical Standardization, 2003.
11. F. Roddier, *Adaptive optics in astronomy*, Cambridge University Press, 1999.
12. E. Dalimier and C. Dainty, "Comparative analysis of deformable mirrors for ocular adaptive optics," *Opt. Express* **13**, pp. 4275–4285, 2005.